

3D Magneto Hydrodynamic Slip Flow of $Al_{50}Cu_{50}$-Water and Cu-Water Nanofluids over a Variable Thickness Stretched Surface

M. Bharath Kumar [1] B. Shanmukha[2]
1.Lecturer in Science, Govt. Polytechnic, Arakere Srirangapatna, Mandya-571401, India.
2.Department of Mathematics, P.E.S College of Engineering, Mandya-571401, India

Abstract
The current paper covers the examination of 3D magneto hydrodynamic nanofluid motion past a slendering (variable thickness) stretching surface under the influence of MHD, Soret and Dufour effects, thermophoresis, Brownian motion and slip impact. For this study, we considered the Cu-water and $Al_{50}Cu_{50}$-water nanofluids past a non-uniform thickness stretching surface. With the help of similarity transformations, we transformed the derived governed equations as ordinary differential equations. The mathematical outcomes determined by employing Runge-Kutta and Newton's methods. We reveal and interpretation the graphs for different parameters like magnetic number, volumetric fraction, Soret number, Dufour number, Brownian motion, thermophoresis parameter, stretching parameter, slip parameters h_1 and h_2. We discussed the skin friction coefficient, reduced Nusselt and reduced Sherwood numbers for the influence of the pertinent parameters with the assistance of tables separately for two nanofluids (Cu-water and $Al_{50}Cu_{50}$-water nanofluids). Results are validated by comparing with the published results and found a favorable agreement.
Keywords: Slip flow, Slendering sheet, Cross diffusion, MHD.

1. Introduction

The study regarding 3D slip flow of MHD heat and mass transfer over stretched sheet has charming the reflection of many researchers owing to its wide demands in industrial and engineering processes. These demands include wire drawing, glass blowing, quick spray cooling, polymer extrusion, metal molding and ice cooler frameworks etc. Nanofluids are deferral of nanoparticles, that illustrate important augmentation of their properties at diffident nanoparticle concentrations. Nanofluid is the mainly desire subject of modern research because of its stunning prospective as far as enhanced heat transfer potential. Nanofluids are fluids with overhanging tinny particles having sizes 1- 100nm. The idea of nanofluid is first initiated by Choi [1]. Wang and Leon [2] presented the application of nanoparticle. The influence of diffusion thermo and thermo diffusion on MHD boundary layer flow towards a stretching surface was studied by Makinde and Aziz [3]. Makinde et al. [4] discussed the effect of convecting heating and buoyancy force on MHD heat transfer flow over stretching surface. The feature of extension in thermal conductivity of the nanofluids was investigated by Masuda et al. [5]. Buongiorno and Hu [6] and Buongiorno[7] discussed the nanofluid application in higher nuclear system and pioneering design of nanofluid flow in the presence of thermophoresis and Brownian motion effects. the boundary layer flow nanofluid flow over astretching surface was explained numerically by Makinde and Aziz [8].

The theoretical study nanofluid flow over a horizontal sheet of a paraboloid revolution with thermal radiation and Lorentz forces was presented by Animasaun and Sandeep [9]. Makinde et al. [10] studied the MHD heat and mass transfer stagnation point flow of a nanofluid towards a stretching surface and solved numerically by Runge-Kutta with shooting method. The influence of magnetic field effect on MHD nanofluids flow over a stretching surface was analyzed by Sheikholeslami et al. [11] and concluded that increasing values of Hartmann number decrease the local Nusselt number. The unsteady MHD mass and heat transfer flow over a vertical cone in the account of cross diffusion effects was presented by Chamkha and El-Kabeir [12]. The study of the heat transfer non-Newtonian nanofluid flow towards a stretching surface with velocity slip condition was studied by Abolbashari et al. [13] and solved analytically by Homotopy Analysis technique.

The dual solution of MHD nanofluid flow towards stretching surface in the presence of thermophoresis effects was investigated by Sandeep and Sulochana [14] and found that rising values of magnetic field parameter enhances the friction factor. Venkateswarlu and SatyaNarayana [15] studied the cross diffusion effects on MHD non-Newtonian fluid flow past a stretching surface. JayachandraBabu and Sandeep [16] explained the heat transfer UCM flow across a melting surface with cross-diffusion and double stratification effects. Soret and Dufour effects on MHD convective flow over a sphere was discussed by Chamkha et al.[17]. Sathish Kumar et al. [18] investigated by free convective MHD Carreau fluid flow past a stretching surface and found that aligned angle parameter have tendency to enhances the reduced Nusselt number. The theoretical study of mass and heat transfer MHD non-Newtonian fluid flow towards a stretching sheet with thermophoresis effect was studied by Sathish Kumar et al. [19]. Kumaran and Sandeep [20] explained the nature of mass and heat transfer MHD fluid flow over a upper paraboloid revolution in the presence of Brownian moment and cross diffusion effects. Recently Sulochana et al [21-22] have studied about the transpiration effect on stagnation-point flow of a carreau nanofluid in the influence of Brownian motion and thermophoresis also authors have invesigated about similarity solution of 3D casson nanofluid flow over a stretching sheet with convective boundary conditions. Very recently Sulochana et al [23-25] explaind the effect of joule heating on a continuously moving thin needle in MHD Sakiadis flow with thermophoresis and Brownian moment, they explained the effect of thermophoresis and Brownian moment on 2D MHD nanofluid flow over an elongated sheet and also they investigated about carreau model for liquid thin film flow of dissipative magnetic-nanofluids over a stretching sheet.

In this investigation, we discussed the effect of Cross diffusion on MHD flow over a stretching surface. Appropriate transformations are used to reduce the governing PDE equations into ODE equations. The influence various pertinent parameters on velocity, temperature and concentration profiles are discussed with the help of graphs.

2. Mathematical formulation

Consider an electrically conducting, incompressible three dimensional flow of nanofluids across a stretching sheet with varying thickness bearing slip effects. The variable thickness of the sheet can be described as $z = A\left(x+y+c\right)^{\frac{1-n}{2}}$. For the sheet become sufficiently thin, we have chosen A is small. We also assumed that the stretched velocity of the sheet is $U_w = a\left(x+y+c\right)^n$ and this is valid for $n \neq 1$ since $n=1$ refers the flat sheet case. We considered the magnetic Reynolds number as low as possible to neglect the induced magnetic field. In this work, we have chosen water as a based fluid comprising of two nanoparticles, namely, Copper (Cu) and Copper Oxide (Cuo). The thermo physical attributes of the nanofluids are taken as described in Table 1. Thermophoresis and Brownian motion effects are taken into account. A magnetic field of strength B_0 is applied to the flow as displayed in Fig.1.

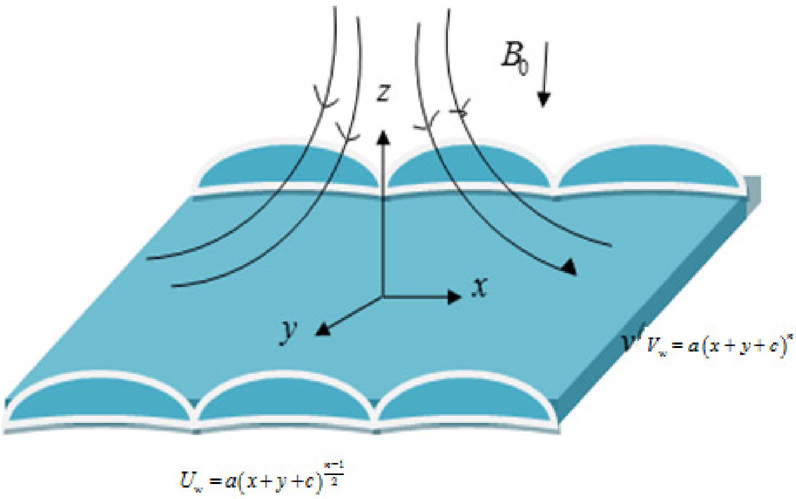

Fig.1 Physical model of the problem

As per the above assumptions, the governing equations are given as follows

$$\frac{\partial u}{\partial x}+\frac{\partial v}{\partial y}+\frac{\partial w}{\partial z}=0, \tag{1}$$

$$\rho_{nf}\left(u\frac{\partial u}{\partial x}+v\frac{\partial u}{\partial y}+w\frac{\partial u}{\partial z}\right)=\mu_{nf}\frac{\partial^2 u}{\partial z^2}-\sigma B^2 u, \tag{2}$$

$$\rho_{nf}\left(u\frac{\partial v}{\partial x}+v\frac{\partial v}{\partial y}+w\frac{\partial v}{\partial z}\right)=\mu_{nf}\frac{\partial^2 v}{\partial z^2}-\sigma B^2 v, \tag{3}$$

$$\left(\rho c_p\right)_{nf}\left(u\frac{\partial T}{\partial x}+v\frac{\partial T}{\partial y}+w\frac{\partial T}{\partial z}\right)=k_{nf}\frac{\partial^2 T}{\partial z^2}+\tau\left(D_B\frac{\partial C}{\partial z}\frac{\partial T}{\partial z}+\frac{D_B}{T_\infty}\left(\frac{\partial T}{\partial z}\right)^2\right)+\frac{D_m K_T}{c_s c_p}\frac{\partial^2 C}{\partial z^2} \tag{4}$$

$$u\frac{\partial C}{\partial x}+v\frac{\partial C}{\partial y}+w\frac{\partial C}{\partial z}=D_B\frac{\partial^2 C}{\partial z^2}+\frac{D_T}{T_\infty}\frac{\partial^2 T}{\partial z^2}+\frac{D_m K_T}{T_m}\frac{\partial^2 T}{\partial z^2} \tag{5}$$

and the representing boundary considerations are

$$\left.\begin{array}{l} u(x,y,z)=U_w(x)+h_1^*\left(\frac{\partial u}{\partial z}\right), v(x,y,z)=V_w(x)+h_1^*\left(\frac{\partial v}{\partial z}\right), \\ T(x,y,z)=T_w(x)+h_2^*\left(\frac{\partial T}{\partial z}\right), C(x,y,z)=C_w(x)+h_3^*\left(\frac{\partial C}{\partial z}\right), \\ \text{and} \\ u=0,\ \text{v=0},\ T=T_\infty\ ,\ C=C_\infty\ at\ \text{z}\to\infty \end{array}\right\} \tag{6}$$

where

$$\xi_1=\frac{k_B T}{\sqrt{2\pi d^2 p}}, h_1^*=\left[\frac{2-f_1}{f_1}\right]\xi_1(x+y+c)^{\frac{1-n}{2}},\ \xi_2=\left(\frac{2\gamma}{\gamma+1}\right)\frac{\xi_1}{\Pr}, \tag{7}$$

$$h_2^*=\left[\frac{2-b}{b}\right]\xi_2(x+y+c)^{\frac{1-n}{2}},\ \xi_3=\left(\frac{2\gamma}{\gamma+1}\right)\frac{\xi_2}{\Pr}, \tag{8}$$

$$h_3^*=\left[\frac{2-d}{d}\right]\xi_3(x+y+c)^{\frac{1-n}{2}},\ B(x)=B_0(x+y+c)^{\frac{n-1}{2}}, \tag{9}$$

$$\left.\begin{array}{l} U_w=a(x+y+c)^n, V_w=a(x+y+c)^n, \tau=\frac{(\rho C_p)_s}{(\rho C_p)_f} \\ T_w=T_\infty+T_0(x+y+c)^{\frac{1-n}{2}}, \text{C}_w=C_\infty+C_0(x+y+c)^{\frac{1-n}{2}} \end{array}\right\}\text{for } n\neq 1 \tag{10}$$

The nanofluid parameters are given by

$$\begin{array}{l} \rho_{nf}=(1-\varphi)\rho_f+\varphi\rho_s, \mu_{nf}=\mu_f/(1-\varphi)^{2.5}, \\ (\rho C_p)_{nf}=(1-\varphi)(\rho C_p)_f+\varphi(\rho C_p)_s, \\ k_{nf}/k_f=\frac{(k_s+2k_f-2\varphi(k_f-k_s))}{(k_s+2k_f+2\varphi(k_f-k_s))}, \end{array} \tag{11}$$

with the utilization of the following similarity transmutations, we changedthe governing equations as ordinary differential equations.

$$\eta=z\sqrt{\frac{(n+1)a}{2\upsilon}}(x+y+c)^{\frac{n-1}{2}} \tag{12}$$

$$T=T_\infty+(T_w(x)-T_\infty)\theta,\ C=C_\infty+(C_w(x)-C_\infty)\phi, \tag{13}$$

$$\left.\begin{array}{l} u=a\ (x+y+c)^n f'(\eta), v=a\ (x+y+c)^n g'(\eta) \\ w=-\sqrt{\frac{2a\nu}{n+1}}(x+y+c)^{\frac{n-1}{2}}\left[\frac{n+1}{2}(f+g)+\ \eta\ \left(\frac{n-1}{2}\right)(f'+g')\right] \end{array}\right\} \tag{14}$$

By using eqs. (11)- (14), the equations (2)-(5) changed as the below differential equations:

$$A\left(\frac{n+1}{2}\right)f'''-B\left(nf'^2+nf'g'-\frac{n+1}{2}(f+g)f''\right)-Mf'=0, \tag{15}$$

$$A\left(\frac{n+1}{2}\right)g'''-B\left(ng'^2+nf'g'-\frac{n+1}{2}(f+g)g''\right)-Mg'=0, \tag{16}$$

$$\frac{k_{nf}}{k_f}\theta''+Nb\theta'\phi'+Nt\theta'^2+Du\,\phi''-\frac{2}{n+1}\Pr C\left(\frac{1-n}{2}(f'+g')\theta-\frac{n+1}{2}(f+g)\theta'\right)=0, \tag{17}$$

$$\phi''+\frac{Nt}{Nb}\theta''+\mathrm{Sr}\,\theta''-Le\left(\frac{1-n}{1+n}(f'+g')\phi-(f+g)\phi'\right)=0 \tag{18}$$

where the constants $A, B,$ and C can be given as

$$A=\frac{1}{(1-\varphi)^{2.5}},\ B=\left((1-\varphi)+\varphi\frac{\rho_s}{\rho_f}\right),\ C=\left((1-\varphi)+\varphi\frac{(\rho C_p)_s}{(\rho C_p)_f}\right)$$

and the representing boundary considerations are

$$\left.\begin{array}{l} f(0)=\lambda\left(\frac{1-n}{n+1}\right)\left[1+h_1 f''(0)\right], f'(0)=\left[1+h_1 f''(0)\right],\\ g(0)=\lambda\left(\frac{1-n}{n+1}\right)\left[1+h_1 g''(0)\right], g'(0)=\left[1+h_1 g''(0)\right],\\ \theta(0)=\left[1+h_2\theta'(0)\right],\phi(0)=\left[1+h_3\phi'(0)\right],\\ f'(\infty)=0, g'(\infty)=0,\theta(\infty)=0,\phi(\infty)=0, \end{array}\right\} \tag{19}$$

where M, $\Pr$, Nb, Nt, Le, λ are specified as

$$\left.\begin{array}{l} M=\frac{\sigma B_0^2}{\rho_f a},\Pr=\frac{\mu C_p}{k},\lambda=A\sqrt{\frac{(n+1)a}{2\upsilon}},Sr=\frac{D_m K_T(T_w-T_\infty)}{T_w D_B(C_w-C_\infty)},\\ Du=\frac{D_m K_T(C_w-C_\infty)}{\rho\upsilon C_s C_p(T_w-T_\infty)},Nb=\frac{\tau D_B(C_w-C_\infty)}{(\mu C_p)_f},Nt=\frac{\tau D_T(T_w-T_\infty)}{T_\infty(\mu C_p)_f},Le=\frac{\upsilon_f}{D_B} \end{array}\right\} \tag{20}$$

For engineering concern, the skin-friction coefficient, the localNusselt and the Sherwood numbers (after non-dimensionalization) are given by

$$\left.\begin{array}{l} C_f=2\left(\frac{n+1}{2}\right)^{0.5}(\mathrm{Re}_x)^{-1/2}f''(0).\ Nu_x=-\left(\frac{n+1}{2}\right)^{0.5}(\mathrm{Re}_x)^{1/2}\theta'(0)\\ \mathrm{Sh}_x=-\left(\frac{n+1}{2}\right)^{0.5}(\mathrm{Re}_x)^{1/2}\phi'(0) \end{array}\right\} \tag{21}$$

where Re_x is the local Reynolds number defined as $\mathrm{Re}_x=\frac{U_w(x)(x+y+c)}{\upsilon_f}$

4. Results and discussion

The mathematical outcomes Eqs. (15)-(18) with the boundary conditions Eq. (19) are solved by employing Runge-Kutta and Newton's methods. The behavior of magnetic field measured on velocity in x and y directions, temperature and concentration are distributed in Figs. 2 – 5. It is clear that the larger values of magnetic field lesser the flow of velocity in x and y direction and boosting the concentration field but in temperature field the flow is enhances somewhere after that its reverse. Generally, supremacy of magnetic field develops the resistance force. This force diminish the velocity in x and y directions and enlarge the concentration field. As seen, Cu ware nanofluid highly upgrades by the resistive flow when comparing with $Al_{50}Cu_{50}$-water nano fluid in concentration field.

Growing the values of volumetric fraction on velocity, temperature and concentration is displays in Figs. 6 – 9. It is shown that rising the values of volumetric fraction diminish the velocity flow in x and y directions but enhances the thermal and concentration fields. Usually, rising the volumetric fraction of nano particles enlarge the thermal and concentration boundary layers thickness. This enlargement causes to shift the particles over from the surface. From Figs. 10 & 11 shows the enlarging values of soret number grows the thermal and concentration profiles. It is evident that the boosting of soret number increases the thermal and concentration boundary layers.

Fig. 12 represent the temperature filed for rising values of Dufour number. It is seen that enhances of Dufour number boost up the thermal boundary layer. Brownian motion effects displayed in temperature and concentration profiles in Figs. 13 and 14. It is observed that higher values of Brownian motion grows the thermal boundary layer but its opposite in concentration field. Figs. 15 and 16 respectively establish the different values of thermophoresis parameter over the temperature and concentration fields. We observe that rising the thermal and concentration boundary layers with growing the values of Nt. Generally thermal boundary layer density enlarges the thermopesis parameter.

Figs. 17 – 22 are elucidates the impact of slip parameters h_1 and h_2 through velocity, temperature and concentration fields. It is percebtible that an asending in h_1 the temperature and concentration boundary layers are also an asending but its reversible in h_2. Influence of stretching ratio parameter of velocity in x and y directions, temperature and concentration distributions are displayed in Figs. 23 – 26. Rising the values of stretching parameter shrinking the velocity in x and y directions, thermal and concentration boundary layers. In generally, stretching parameter boosts automatically the flow pressure enhance to this reason.

Tables 1 and 2 depict the variations in the wall friction, local Nusselt and Sherwood numbers at different pertinent parameters for $Al_{50}Cu_{50}$-water and Cu -water nanofluids respectively. It is clear that the increasing values of M and ϕ declines the heat and mass transfer rate along with wall friction of both fluids. The rising values of Soret and thermophoresis parameters suppress the mass and heat transfer rate. A reverse trend has been observed for boosting values of Dufour number. Increasing values of Brownian moment and slip parameters showed mixed response in heat and mass transfer performance.

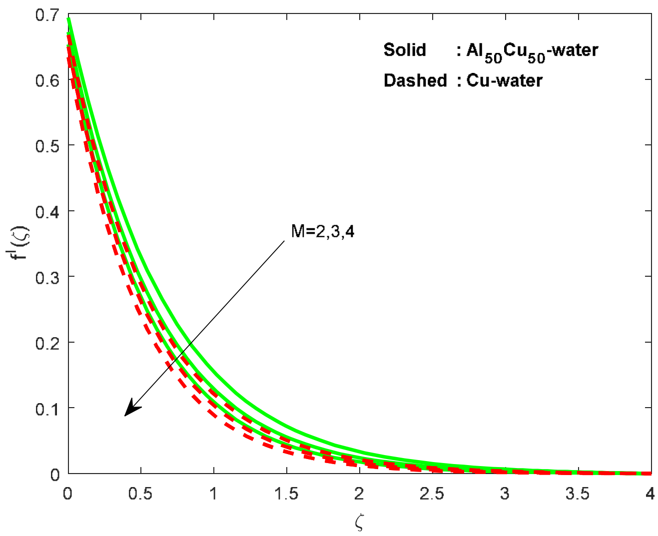

Fig. 2 Effect of magnetic field parameter on velocity profile.

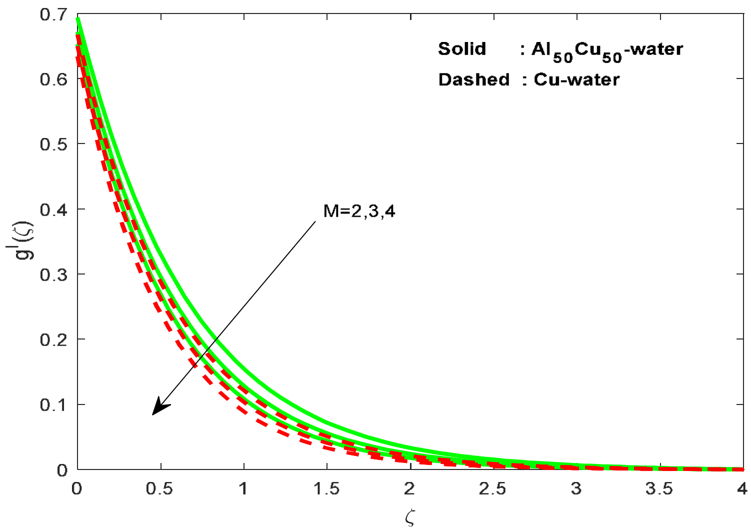

Fig. 3 Effect of magnetic field parameter on velocity profile.

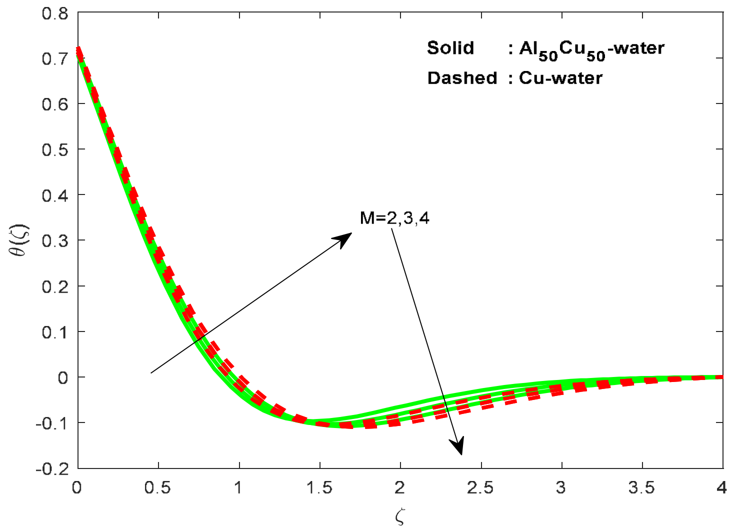

Fig. 4 Effect of magnetic field parameter on temperature profile.

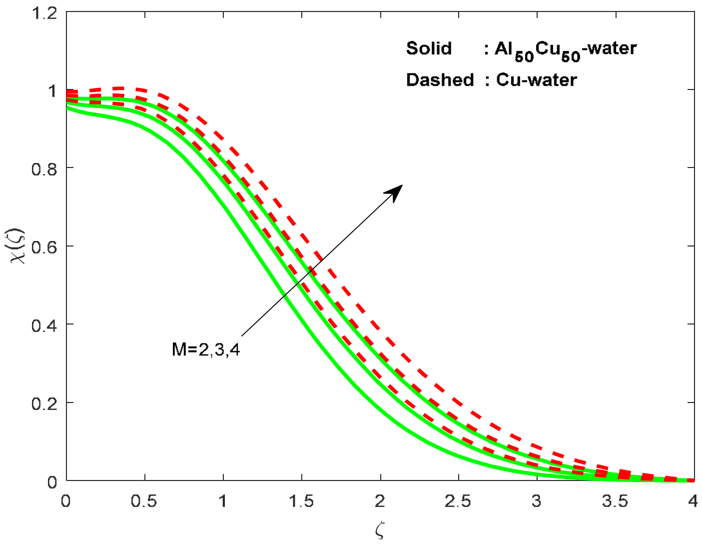

Fig. 5 Effect of magnetic field parameter on concentration profile.

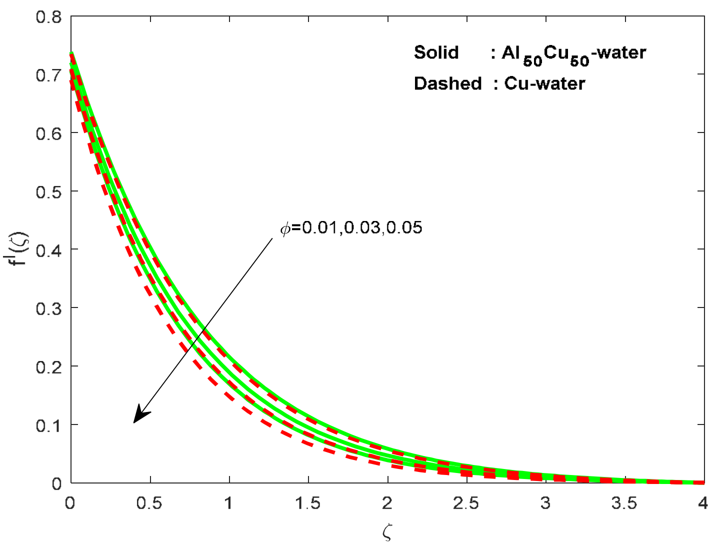

Fig. 6 Effect of volumetric fraction on velocity profile.

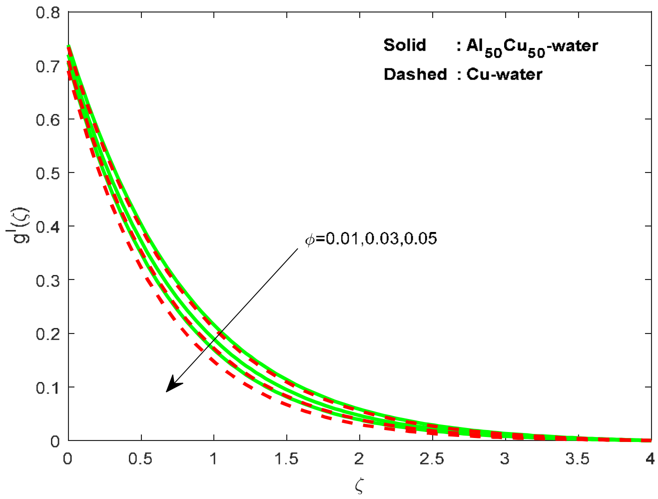

Fig. 7 Effect of volumetric fraction on velocity profile.

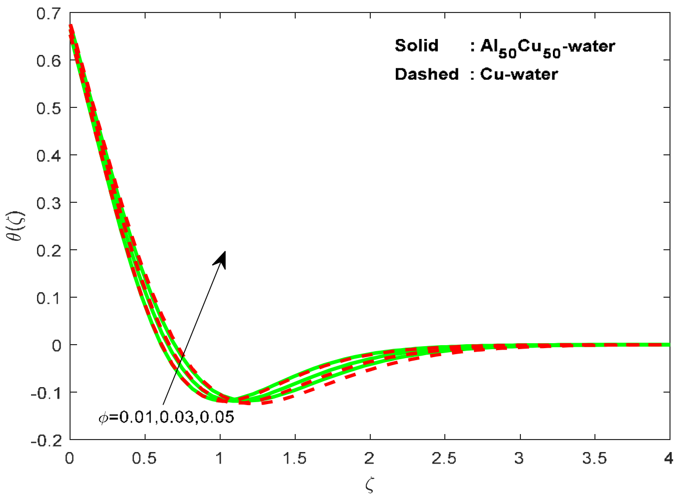

Fig. 8 Effect of volumetric fraction on temperature profile.

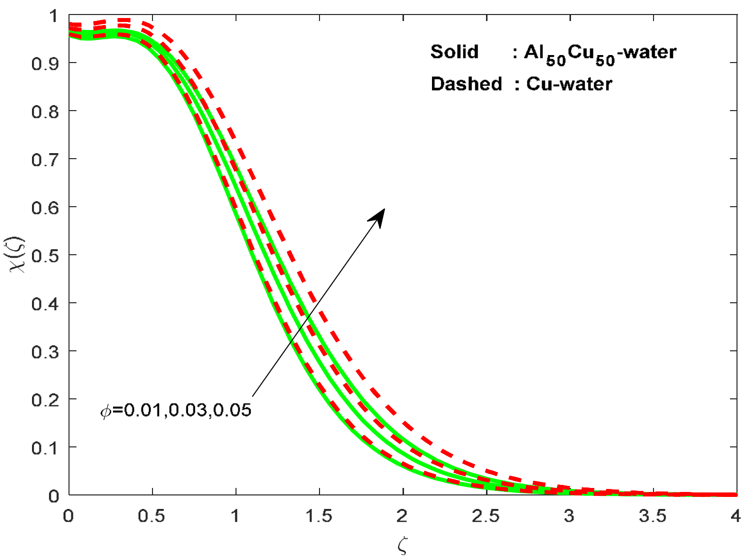

Fig. 9 Effect of volumetric fraction on concentration profile.

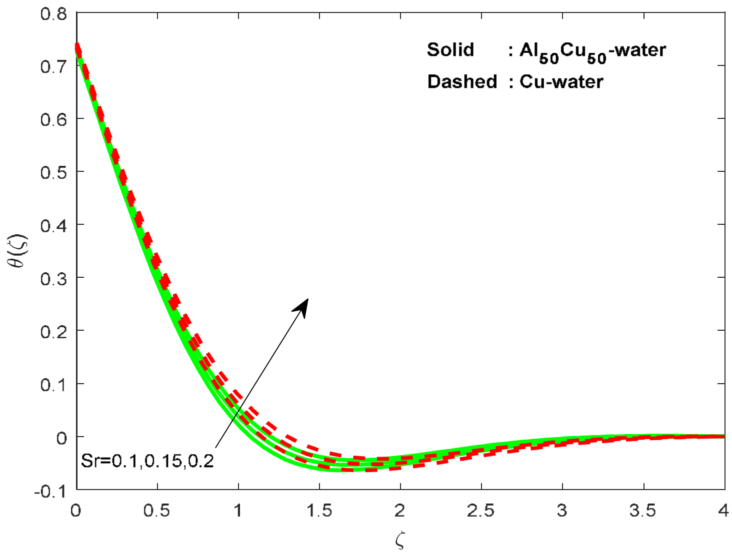

Fig. 10 Effect of Soret number on temperature profile.

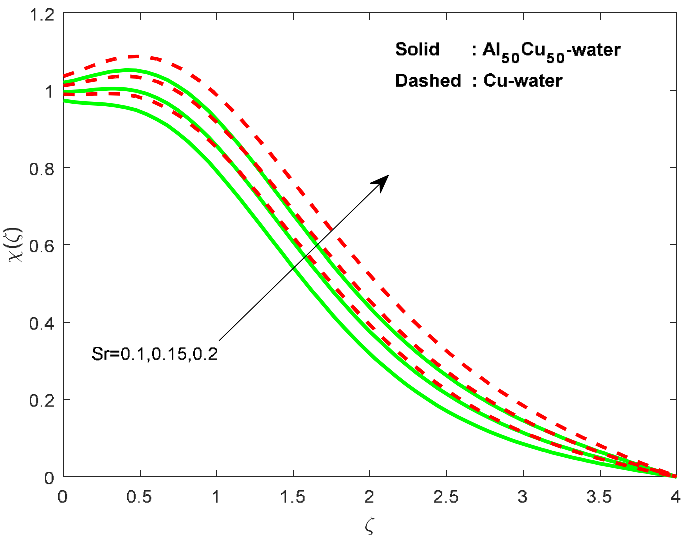

Fig. 11 Effect of Soret number on concentration profile

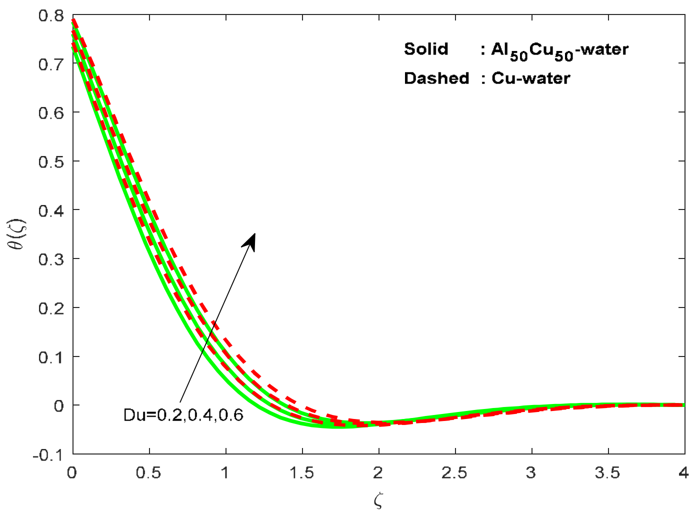

Fig. 12 Effect of Dufour number on temperature profile.

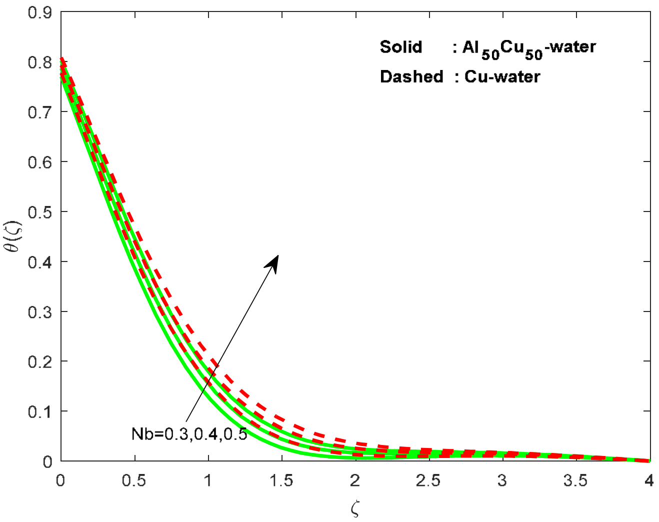

Fig. 13 Effect of Brownian motion parameter on temperature profile.

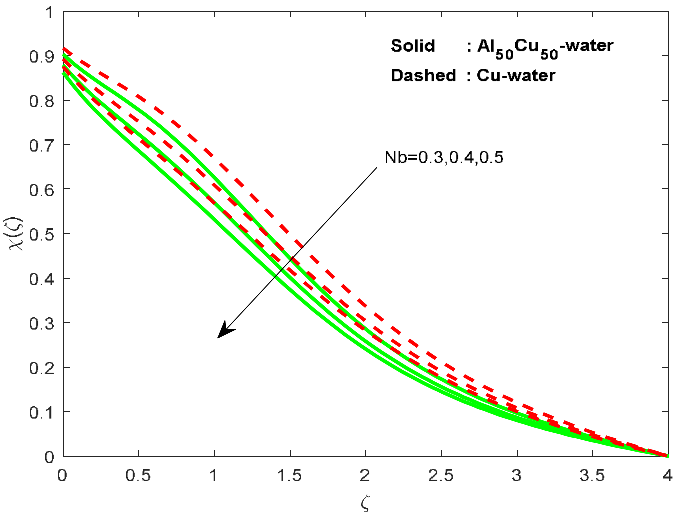

Fig. 14 Effect of Brownian motion parameter on concentration profile.

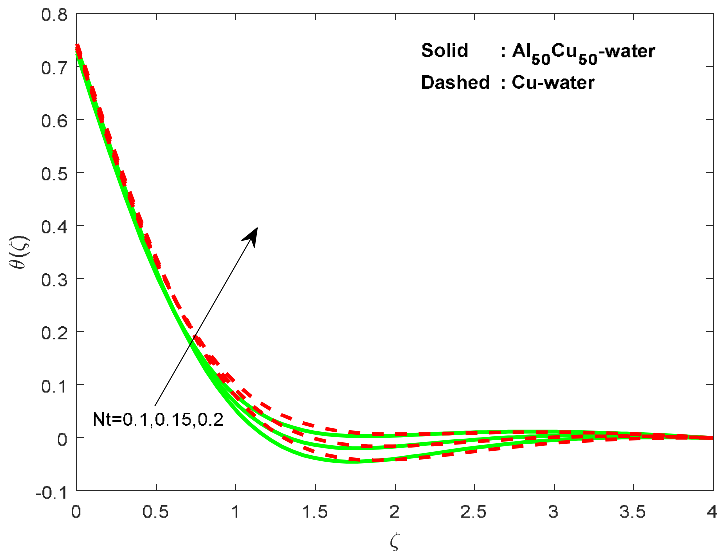

Fig. 15 Effect of thermophoresis parameter on temperature profile.

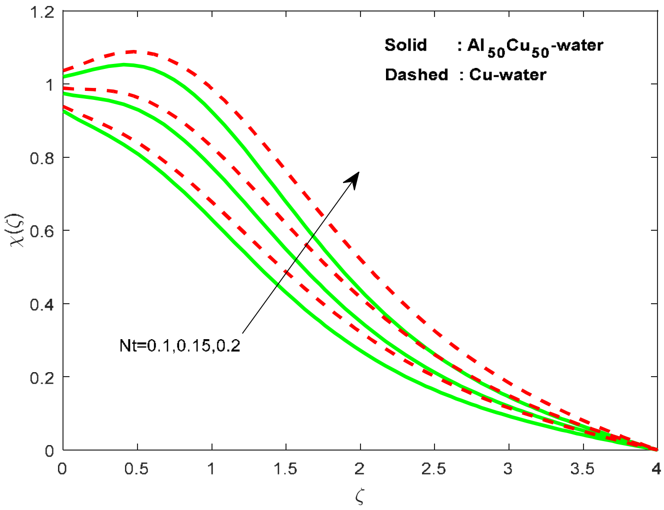

Fig. 16 Effect of thermophoresis parameter on concentration profile.

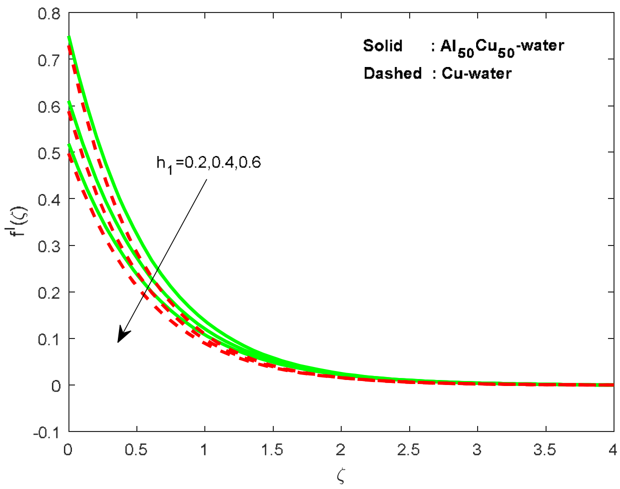

Fig. 17 Effect of slip parameter (h_1) on velocity profile.

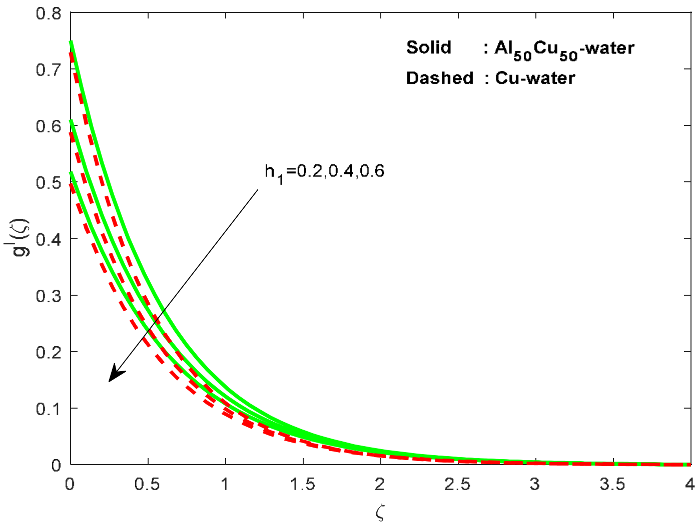

Fig. 18 Effect of slip parameter (h_1) on velocity profile.

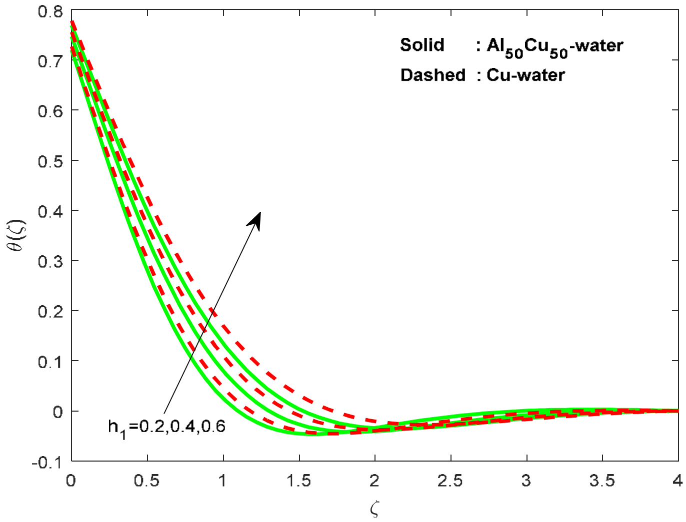

Fig. 19 Effect of slip parameter (h_1) on temperature profile.

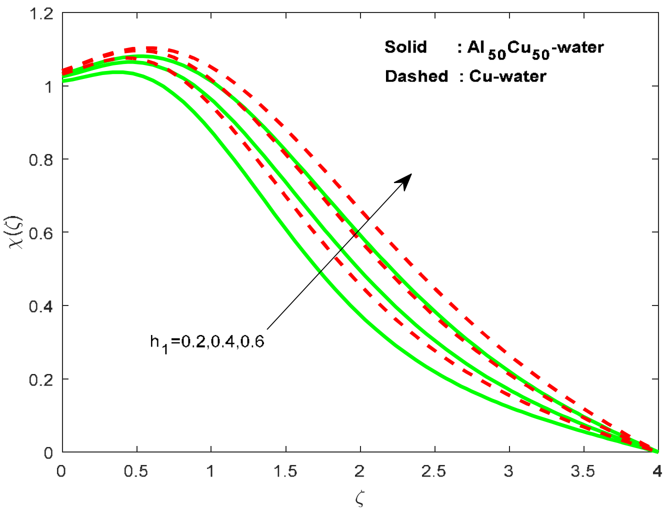

Fig. 20 Effect of slip parameter (h_1) on concentration profile.

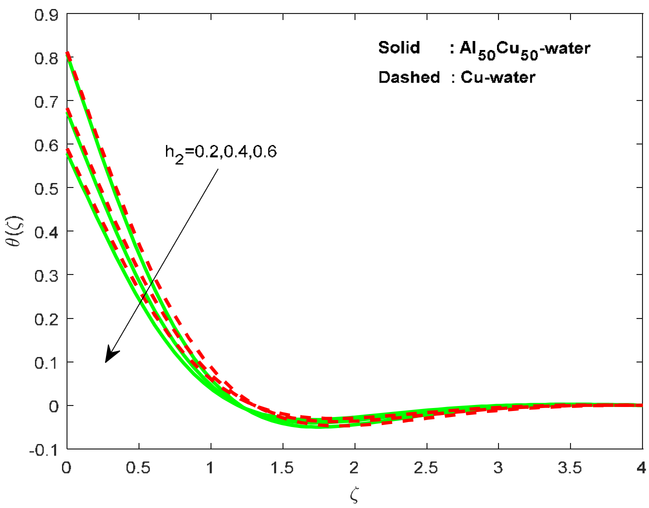

Fig. 21 Effect of slip parameter (h_2) on temperature profile.

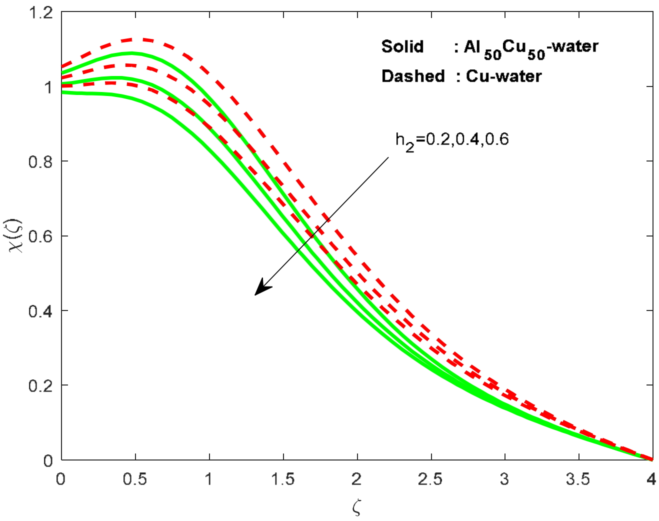

Fig. 22 Effect of slip parameter (h_2) on concentration profile.

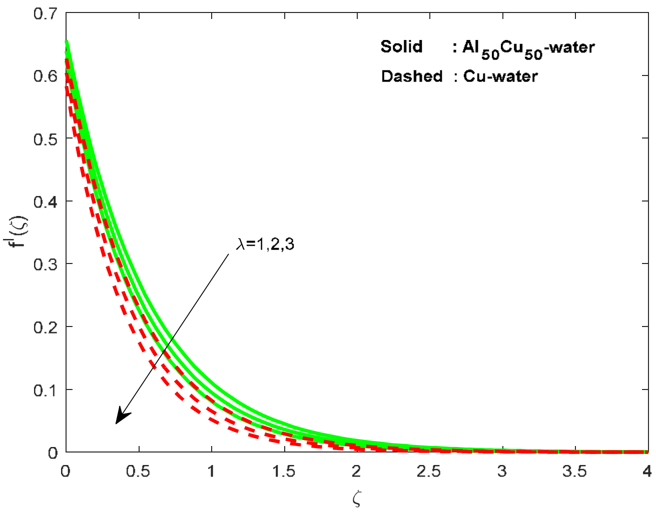

Fig. 23 Effect of stretching ration parameter on velocity profile.

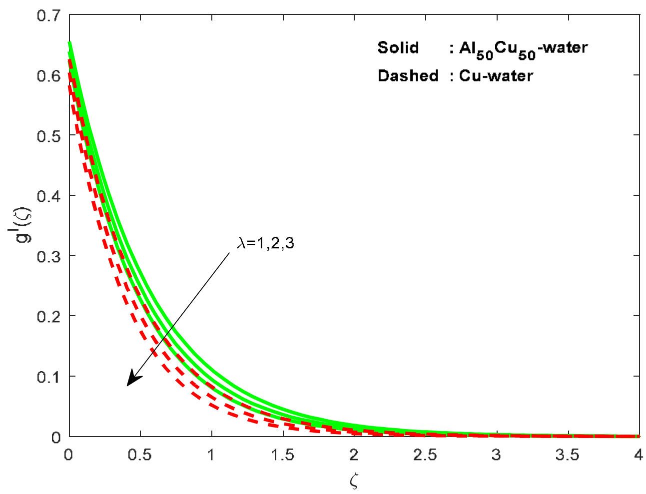

Fig. 24 Effect of stretching ration parameter on velocity profile.

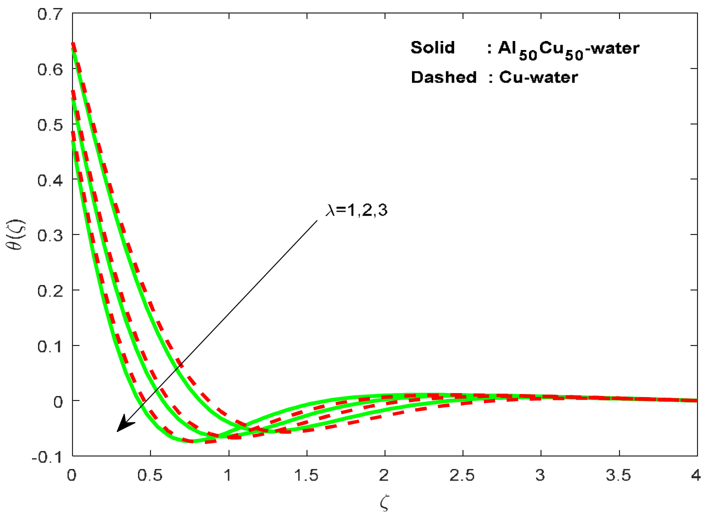

Fig. 25 Effect of stretching ration parameter on temperature profile.

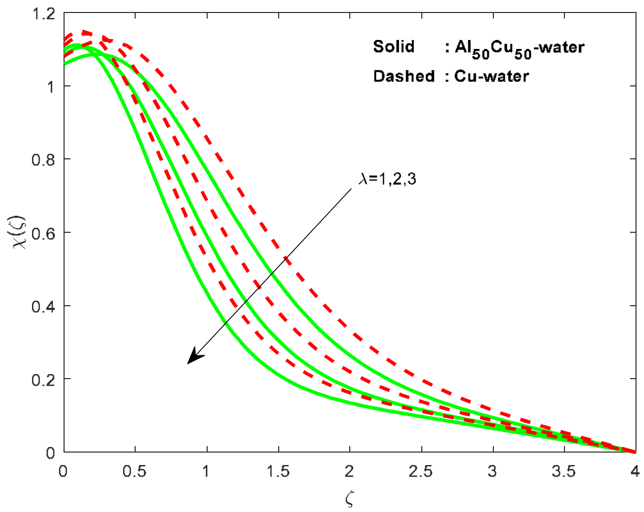

Fig. 26 Effect of stretching ration parameter on concentration profile.

Table-1: Impact of some flow modifying quantites on friction factors, Nusselt and shearwood number for $Al_{50}Cu_{50}$ -water nanofluid.

M	ϕ	Sr	Du	Nb	Nt	h_1	h_2	λ	$f^{//}(0)$	$-\theta'(0)$	$-\phi'(0)$
2									-1.020172	0.978514	0.154037
3									-1.093088	0.956584	0.106622
4									-1.156323	0.935714	0.065714
	0.01								-0.873383	1.158138	0.146547
	0.03								-0.933652	1.124555	0.123105
	0.05								-0.980647	1.091920	0.107653
		0.1							-1.093088	0.911126	0.086443
		0.15							-1.093088	0.898059	0.012120
		0.2							-1.093088	0.884880	-0.066199
			0.2						-1.093088	0.884880	-0.066199
			0.4						-1.093088	0.799575	0.007754
			0.6						-1.093088	0.718023	0.078352
				0.3					-1.093088	0.766785	0.322305
				0.4					-1.093088	0.712041	0.403186
				0.5					-1.093088	0.659477	0.458732
					0.1				-1.093088	0.918169	0.246307
					0.15				-1.093088	0.902131	0.086781
					0.2				-1.093088	0.884880	-0.066199
						0.2			-1.248978	0.933268	-0.042795
						0.4			-0.973933	0.842518	-0.083565
						0.6			-0.802623	0.770015	-0.104465
							0.2		-1.093088	0.966331	-0.118110
							0.4		-1.093088	0.814838	-0.021318
							0.6		-1.093088	0.701420	0.051821
								1	-1.148792	1.208251	-0.196707
								2	-1.203467	1.505983	-0.284143
								3	-1.256161	1.763562	-0.324511

Table-2: Impact of some flow modifying quantites on friction factors, Nusselt and shearwood number for Cu-water nanofluid.

M	ϕ	Sr	Du	Nb	Nt	h_1	h_2	λ	$f^{//}(0)$	$-\theta'(0)$	$-\phi'(0)$
2									-1.08357	0.958712	0.086519
3									-1.167716	0.938595	0.049151
4									-1.220673	0.918785	0.017713
	0.01								-0.885487	1.156239	0.138052
	0.03								-0.907333	1.118538	0.095131
	0.05								-1.032835	1.083005	0.066721
		0.1							-1.167716	0.888982	0.032987
		0.15							-1.167716	0.874190	-0.042069
		0.2							-1.167716	0.859120	-0.120981
			0.2						-1.167716	0.859120	-0.120981
			0.4						-1.167716	0.776123	-0.047472
			0.6						-1.167716	0.696775	0.022751
				0.3					-1.167716	0.743978	0.277133
				0.4					-1.167716	0.690812	0.359499
				0.5					-1.167716	0.639767	0.415991
					0.1				-1.167716	0.888537	0.203704
					0.15				-1.167716	0.874341	0.038895
					0.2				-1.167716	0.859120	-0.120981
						0.2			-1.352363	0.910572	-0.105040
						0.4			-1.030272	0.814535	-0.130681
						0.6			-0.837795	0.73915	-0.137009
							0.2		-1.167716	0.937014	-0.173551
							0.4		-1.167716	0.792048	-0.075528
							0.6		-1.167716	0.683206	-0.001409
								1	-1.245642	1.176118	-0.268380
								2	-1.320550	1.463693	-0.268380
								3	-1.393912	1.709909	-0.413606

5. Conclusions

Three-dimensional magnetohydrodynamic nanofluid flow past a slendering (variable thickness) stretching surface under the influence of thermophoresis, Brownian motion and cross diffusion effects are studied numerically. The numerical outputs are summarized as follows:

- The heat and mass transfer rate is high in $Al_{50}Cu_{50}$-water nanofluid when equated with Cu-water nanofluid.
- Cross diffusion, thermophoresis and Brownian moment effects regulates the thermal and species fields.
- Rising the volume fraction of nanoparticles decline the local Nusselt and Sherwood numbers.
- Cu-water is highly influenced by the Lorentz force when compared with the $Al_{50}Cu_{50}$-water nanofluid.
- Flow, thermal and concentration fields of $Al_{50}Cu_{50}$-water and Cu-water nanofluids are not uniform.

References

[1] S. U. S. Choi, Enhancing thermal conductivity of fluids with nanoparticles, The proceedings of the 1995 ASME International Mechanicle Engineering Congrss and Exposition, 66 (1995) 99-105.

[2] K. V. Wang, O. D. Leon, Application of nanofluid: current and future, Ad. Mech. Eng.(2010) 519659.

[3] O. D. Makinde, A. Aziz, Boundary layer flow of a nanofluid past a stretching sheet with convective boundary condition, Int. J. Therm. Sci. 50 (2011) 1326-1332.

[4] O. D. Makinde, W. A. Khan, Z. H. Khan, Buoyancy effects on MHD stagnation point flow and heat transfer of a nanofluid past a convectively heated stretching/shrinking sheet, Int. J. of Heat and Mass Transfer 62 (2013) 526-533.

[5] H. Masuda, A. Ebata, K. Teramae, N. Hishinuma, Alteration of thermal conductivity and viscosity of liquid by dispersing ultra-fine particles, NetsuBussei 7 (1993) 227-233.

[6] J. Buongiorno, W. Hu, in proceedings of international congress on Advances in Nuclear Power Plants (Carran Associate, Inc., Seoul), 5705 (2005).

[7] J. Buongiorno, Convective transport in nanofluids, J. Heat Transfer, 128 (2006) 240-250.

[8] O. D. Makinde, A. Aziz, Boundary layer flow of a nanofluid past a stretching sheet with convective boundary condition, Int. J. Ther. Sci. 50 (2011) 1326-1332.

[9] I. L. Animasaun , N. Sandeep, Buoyancy induced model for the flow of 36 nm alumina-water nanofluid along upper horizontal surface of a paraboloid of revolution with variable thermal conductivity and viscosity, Powder Technology 301 (2016) 858-867.

[10] O. D. Makinde, W. A. Khan, Z. H. Khan, Buoyancy effects on MHD stagnation point flow and heat transfer of a nanofluid past a convectively heated stretching/shrinking sheet, Int. J. Heat Mass Tran. 62 (2013) 526-533.

[11] M. Sheikholeslami,M.M. Rashidi, D. D. Ganji, Effects of non-uniform magnetic field on forced convection heat transfer of Fe_3O_4 -water nanofluid, Comput.Methods Appl. Mech. Engrg. 294 (2015) 299-312.

[12] A. J. Chamkha, S. M. M. El-Kabeir, Unsteady heat and mass transfer by MHD mixed convection flow from a rotating vertical cone with chemical reaction and Soret and Dufour effects, Che. Eng. Comm. 200 (2013) 1220-1236.

[13] M. H. Abolbashari,N. Freidoonimehr,F. Nazari,M. M. Rashidi, Analytical modelling of entropy generation for Cassonnano-fluid flow induced by a stretching surface, Advanced Powder Tech.26(2015) 542-552.

[14] N. Sandeep, C. Sulochana, Dual solution of radiative MHD nanofluid flow over an exponentially stretching sheet with heat generation/absorption, Applied Nanoscience, 6 (2016) 131-139.

[15] B. Venkateswarlu, P. V. SatyaNarayana, Soret and Dufour effects on MHD flow of a Maxwell fluid over a stretching sheet with Joule heating, FHMT, 9 (2017) 11.

[16] M. JayachandraBabu, N. Sandeep, UCM flow across a melting surface in the presence of double stratification and cross-diffusion effects, J. of Molecular Liquids, 232 (2017), 27-35.

[17] A. J. Chamkha, A. M. Aly, Z. A. S. Raizah, Double-Diffusion MHD Free convective flow along a sphere in the presence of a homogeneous chemical reaction and Soret and Dufour effects, Appl. and Com. Math. 6 (2017) 34-44.

[18] M. Sathish Kumar, N. Sandeep, B. Rushi Kumar, Free convective heat transfer of MHD dissipative Carreau nanofluid flow over a stretching sheet, FHMT, 8 (2017) 13.

[19] M. Sathish Kumar, N. Sandeep, B. Rushi Kumar, S. Saleem, A comparative study of chemically reacting 2D flow of Casson and Maxwell fluids, Alexandria Eng. J. (2017).

[20] G. Kumaran, N. Sandeep, Thermophoresis and Brownian motion moment effects on parabolic flow of MHD Casson and Williamson fluids with cross diffusion, J. of Mole. L. 233 (2017) 262-269.

[21] C. Sulochana, G.P. Ashwinkumar, N. Sandeep, Transpiration effect on stagnation-point flow of a Carreau nanofluid in the presence of thermophoresis and Brownian motion, Alexandria Engineering Journal. 55 (2016) 1151-1157.

[22] C. Sulochana, G.P. Ashwinkumar, N. Sandeep, Similarity solution of 3D Casson nanofluid flow over a stretching sheet with convective boundary conditions, Journal of the Nigerian Mathematical Society. 35 (2016) 128–141.

[23] C. Sulochana, G.P. Ashwinkumar, N. Sandeep, Joule heating effect on a continuously moving thin needle in MHD Sakiadis flow with thermophoresis and Brownian moment, The European Physical Journal Plus. 132: 387 (2017).

[24] C. Sulochana, G.P. Ashwinkumar, N. Sandeep, Effect of Thermophoresis and Brownian Moment on 2D MHD Nanofluid Flow over an Elongated Sheet, Defect and Diffusion Forum. 377 (2017) 111-126.

[25] C. Sulochana, G.P. Ashwinkumar, Carreau Model for Liquid Thin Film Flow of Dissipative Magnetic-Nanofluids over a Stretching Sheet, International Journal of Hybrid Information Technology. 10 (2017) 239-254.